**TCF7L2 is a terminal selector that regulates postmitotic differentiation programs and excitability patterns in the thalamus**

Marcin Andrzej Lipiec,[1,2] Kamil Koziński,[1] Tomasz Zajkowski,[1] Michał Dąbrowski,[3] Chaitali Chakraborty,[1] Joanna Urban-Ciećko,[3] Angel Toval,[4] José Luis Ferran,[4] Andrzej Nagalski,[1] Marta Barbara Wiśniewska[1,*]

1. Centre of New Technologies, University of Warsaw, Poland
2. Faculty of Biology, University of Warsaw, Poland
3. Nencki Institute of Experimental Biology, Warsaw, Poland
4. Department of Human Anatomy and Psychobiology, School of Medicine, University of Murcia, Spain

*Correspondence should be addressed to Marta B. Wiśniewska, Centre of New Technologies, University of Warsaw; Banacha 2c, 02-097 Warsaw, Poland; m.wisniewska@cent.uw.edu.pl; +(48) 22 554-36-90

Running title: Role of TCF7L2 in thalamic differentiation and excitability

**Abstract**

The thalamus and habenula integrate sensory information, adaptive task control, and reward processing. Their postmitotic differentiation and establishment of their electrophysiological properties are not well understood. The present study investigated the role of the thalamo-habenular-specific transcription factor TCF7L2 in molecular and functional development of this region. In *Tcf7l2* knockout embryos, expression of the postmitotic pan-thalamic and pan-habenular selectors *Gbx2* and *Pou4f1*, respectively, was not maintained, and cell adhesion and axon guidance genes were downregulated. Neurons adopted proper neurotransmitter fate, but they did not segregate to form separate nuclei and did not grow axons toward their targets, and their afferent connections were disorganised. When *Tcf7l2* was knocked out postnatally, thalamus-specific voltage-gated ion channel genes were not induced, and burst and tonic spiking in thalamic neurons was strongly reduced. These findings indicate that TCF7L2 functions as a master and versatile terminal selector in the thalamo-habenular region to regulate the morphological differentiation and molecular divergence of cells during embryogenesis and the establishment of postnatal thalamic intrinsic excitability. These results provide new insights into regulatory principles of neuronal terminal differentiation in vertebrates.

**Keywords**

neuronal excitability, brain, development, terminal selector, Wnt signalling

## Introduction

The thalamus is a sensory relay centre, and part of the cortico-subcortical neural loops that process sensorimotor information and produce goal-directed behaviours (Ribary U 2005; Sherman SM 2017; Lien AD and M Scanziani 2018). The habenula controls reward- and aversion-driven behaviours by connecting the prefrontal cortex, limbic system, and basal ganglia with the monoamine system in the brainstem (Hikosaka O 2010; Benekareddy M et al. 2018). Anatomical abnormalities and disconnectivity of the thalamus and habenula are implicated in schizophrenia, autism spectrum disorder, Tourette syndrome, obsessive-compulsive disorder, and depression (Kobayashi Y et al. 2013; Pergola G et al. 2015; Fakhoury M 2017). Knowledge of thalamic and habenular development and functioning is required to fully understand the aetiology of these psychiatric conditions, but such information is currently limited.

During postmitotic differentiation, thalamic and habenular neurons segregate into discrete nuclei, develop specific molecular identities (Vue TY et al. 2009; Scholpp S and A Lumsden 2010; Nagalski A, L Puelles, et al. 2016; Gezelius H and G Lopez-Bendito 2017; Gezelius H et al. 2017) and extend axons toward their targets (Hikosaka O et al. 2008; Price DJ et al. 2012; Antón-Bolaños N et al. 2018). These processes are presumably regulated by prosomere 2-specific postmitotic transcription factors. *Gbx2* is an early specific marker of the thalamic mantle zone (Li K et al. 2012; Mallika C et al. 2015), whereas the expression of *Pou4f1* marks postmitotic habenula neurons (Quina LA et al. 2009; Serrano-Saiz E et al. 2018). Both transcription factors were shown to be critically required for the establishment of molecular identities in the thalamus and habenula, respectively, as well as the survival of neurons. GBX2 was shown to play an essential role in thalamocortical axon growth (Miyashita-Lin EM et al. 1999; Hevner RF et al. 2002; Chen L et al. 2009; Chatterjee M et al. 2012) whereas the growth of habenulo-interpeduncular axons is not controlled by POU4F1 (Quina LA *et al.* 2009;

Serrano-Saiz E *et al.* 2018). In addition to *Gbx2* and *Pou4f1*, newly generated prosomere 2 neurons in different subregions induce the expression of several dozen marker genes, such as *Rora*, *Foxp2* and *Nr4a2* (Quina LA *et al.* 2009; Suzuki-Hirano A et al. 2011; Gezelius H *et al.* 2017), which together generate combinatorial codes of transcription factors in the thalamus and habenula (Nagalski A, L Puelles*, et al.* 2016) and regulate some aspects of postmitotic differentiation in prosomere 2 (Quina LA *et al.* 2009; Ebisu H et al. 2016; Vitalis T et al. 2017).

Neurons in thalamic and habenular regions progressively acquire electrophysiological characteristics postnatally (Yuge K et al. 2011), but the way in which this process is regulated is not well understood. POU4F1 was recently identified as a selector of glutamatergic neurons in the medial habenula, where it maintains the expression of the glutamate transporter gene *Vglut1* (*Slc17a7*), but the impact of *Pou4f1* knockout on electrophysiological responses of cells in this region was not functionally tested (Serrano-Saiz E *et al.* 2018). Terminal selectors of thalamic excitability profiles are unknown. GBX2 cannot serve as such a regulator because its expression does not persist in most thalamic nuclei until late gestation or early postnatal stages (Li K *et al.* 2012) when electrophysiological maturation occurs in the thalamus.

*Tcf7l2* encodes a member of the LEF1/TCF family of transcription factors (Cadigan KM and ML Waterman 2012) and is the only shared marker of both the habenula and thalamus (Nagalski A et al. 2013; Nagalski A, L Puelles*, et al.* 2016; Lee M et al. 2017). However, the function of *Tcf7l2* in the postmitotic development of these regions has only begun to be investigated in zebrafish (Beretta CA et al. 2013; Husken U et al. 2014) and mice (Lee M *et al.* 2017). In *Tcf7l2*$^{-/-}$ mice, some postmitotic markers were mis-expressed in the prospective thalamus and habenula during neurogenesis, and the formation of thalamocortical and habenulo-interpeduncular tracts was disrupted. The role of TCF7L2 in the anatomical parcellation of this region and maintenance of cell identities and postnatal terminal differentiation has not been investigated. We hypothesized that TCF7L2 might also be involved

in postmitotic differentiation at later stages, based on our previous research that showed the overrepresentation of thalamic genes within *in silico*-identified putative targets of this transcription factor (Wisniewska MB et al. 2012; Nagalski A, L Puelles*, et al.* 2016).

The present study used both total and conditional knockout mice to investigate the role of *Tcf7l2* in the development of the thalamus and habenula at different developmental stages. We found that TCF7L2 is a versatile terminal selector that regulates the overall postmitotic differentiation process in the thalamo-habenular domain and postnatal establishment of electrophysiological characteristics of thalamic neurons.

## Materials and Methods

*Animals.* We used C57BL/6NTac-*Tcf7l2*$^{tm1a}$(EUCOMM)Wtsi/WtsiIeg (*Tcf7l2*$^{tm1a}$) mouse strain (Skarnes WC et al. 2011), with a trap cassette upstream of the critical exon 6 of the *Tcf7l2* gene (Supplementary Fig. 1). For the experimental procedures *Tcf7l2*$^{tm1a/tm1a}$ (*Tcf7l2*$^{-/-}$) and *Tcf7l2*$^{+/+}$ (WT) mice were selected by PCR-based genotyping (Supplementary Table 1). To generate *Cck*$^{Cre}$:*Tcf7l2*$^{fl/fl}$ strain, in which knockout of *Tcf7l2* is induced in the thalamic area between E18.5 and P14 (Characterisation of Cck-IRES-Cre transgene. 2011), *Tcf7l2*$^{tm1a/+}$ animals were first crossed with flippase-expressing mice (JAX stock #009086; (Farley FW et al. 2000)), and then with *Cck*$^{tm1.1(cre)Zjh}$/J mice (*Cck*$^{Cre}$:*Tcf7l2*$^{+/+}$, JAX stock #012706; (Taniguchi H et al. 2011)), which express Cre recombinase from the *Cck* promoter. *Cck*$^{Cre}$:*Tcf7l2*$^{+/+}$ animals were used as WT. Mice were maintained on a 12 h/12 h light/dark cycle with *ad libitum* access to food and water. All of the experimental procedures were conducted in compliance with the current normative standards of the European Community (86/609/EEC) and Polish Government (Dz.U. 2015 poz. 266).

*Brain fixation.* *Tcf7l2*$^{-/-}$ and WT mice were collected on E12.5, E18.5 or P0. Noon on the day of appearance of the vaginal plug was considered E0.5. Timed-pregnant dams were sacrificed by cervical dislocation, the embryos were removed and decapitated. E18.5 and P0 brains were dissected out and fixed overnight in 4% paraformaldehyde (PFA; Cat. no. P6148, Sigma-Aldrich) in 0.1 M phosphate-buffered saline (PBS; pH 7.4; Cat. no. PBS404, BioShop) at 4ºC. E12.5 heads were fixed whole. *Cck*$^{Cre}$:*Tcf7l2*$^{fl/fl}$ and *Cck*$^{Cre}$:*Tcf7l2*$^{+/+}$ mice were sacrificed on P55-P75 (further referred to as P60) by pentobarbital sedation and perfusion with PBS and 4% PFA. Their brains were dissected out and fixed overnight in 4% PFA. For cryostat sections, the brains were sequentially transferred into 15% and 30% sucrose in PBS at 4ºC until they sank. Next, E12.5, E18.5 and P0 tissues were embedded in 10% gelatine/10% sucrose solution in

PBS (Ferran JL et al. 2015, 2015). Postnatal brains were transferred to O.C.T (Cat. no. 4583, Sakura Tissue-Tek). Tissues were frozen in -60ºC isopentane. Sections (20 µm – embryos and P0, 50 µm - adult) were obtained using a Leica CM1860 cryostat. Embryonic and P0 sections were mounted directly on Superfrost-plus slides (Cat. no. J1800AMNZ, Menzel-Gläser). Adult tissue was collected as free-floating sections into an anti-freeze solution (30% sucrose/30% glycerol in PBS). For DiI axon tracing, E18.5 immersion-fixed brains were kept in 4% PFA at 4ºC. Stained sections were visualized under a Nikon Eclipse Ni-U microscope.

*In situ hybridisation.* The hybridisation was performed using digoxigenin-UTP-labelled antisense riboprobes (sense & antisense), synthesized with the DIG RNA labelling Kit (Cat. no. 11175025910, Roche). Plasmids for synthesis of *Foxp2*, *Gad67*, *Gbx2*, *Lef1*, *Prox1, Rora, Tcf7l2*, *Tfap2b* and *Slc17a6* probes come from the collection of José Luis Ferran (Supplementary Table 2). The other plasmids were kind gifts from: James Li from the University of Connecticut Health Center (*Etv1*) (Chatterjee M et al. 2014); Seth Blackshaw from the Johns Hopkins University School of Medicine (*Nkx2-2* and *Sox14*) (Shimogori T et al. 2010); David Price from the University of Edinburgh (*Pax6*) (Walther C and P Gruss 1991) (Supplementary Table 2). Chromogenic *in situ* hybridisation of cryosections was performed as described elsewhere (Ferran JL *et al.* 2015; Puelles L et al. 2016). The stained sections were washed in xylene and mounted using EuKitt (Cat. no. 03989, Sigma-Aldrich). No specific signal was obtained with sense probes (data not shown).

*Fluorescent immunohistochemistry.* Frozen sections were washed in PBS with 0.2% Triton X-100 (PBST) and blocked with 5% normal donkey serum (NDS) for 1 h. The slides were then incubated with primary antibodies mixed in 1% NDS overnight at 4°C. Antibodies against TCF7L2 (1:500; Cat. no. 2569, Cell Signaling), LacZ (1:100; Cat. no. AB986, Merck

Millipore), L1CAM (1:500; Cat. no. MAB5272, Merck Millipore), PAX6 (1:100; Cat. no. PRB-278P, Biolegend), SIX3 (1:100; Cat. no. 200-201-A26S, Rockland), KI-67 (1:100; Cat. no. AB9260, Merck Millipore), TUJ1 (1:65; Cat. no. MAB1637, Merck Millipore), NKX2-2 (1:50; Cat. no. 74.5A5, DSHB), POU4F1 (1:300; (Fedtsova NG and EE Turner 1995)) were used. Sections were then incubated for 1 h with appropriate secondary antibody conjugated with Alexa Fluor 488 or 594 (1:500; Cat. no. A-21202, A-21207, and A-11076, ThermoFisher Scientific). The slides were additionally stained with Hoechst 33342 (1:10000; Cat. no. 62249, ThermoFisher Scientific), washed and mounted with Vectashield Antifade Mounting Medium (Cat. no. H1000, Vector Laboratories).

*DAB immunohistochemistry*. Free-floating sections were washed in PBST, incubated in 0.3% $H_2O_2$ for 10 min, blocked with 3% normal goat serum (NGS) for 1 h and incubated with primary antibodies against TCF7L2 (1:1000) or POU4F1 (1:600) in 1% NGS overnight at 4ºC. Next, sections were incubated for 1 h with biotinylated goat anti-rabbit antibody (Cat. no. BA-1000, Vector Laboratories) in 1% NGS, and then for 1 h in Vectastain ABC reagent (Cat. no. PK-6100, Vector Laboratories). Staining was developed using 0,05% DAB (Cat. no. D12384, Sigma-Aldrich) and 0.01% $H_2O_2$. Next, sections were mounted onto Superfrost plus slides, washed in xylene and mounted using EuKitt .

*DiI axon tracing.* PFA-fixed brains were separated into hemispheres and small DiI crystals (Cat. no. D-3911, ThermoFisher Scientific) were placed in the exposed thalamic surface. Tissue was then incubated in 4% PFA at 37ºC for 18-21 days. The hemispheres were then embedded in 5% low-melting-point agarose and cut into 100 µm thick coronal sections in a vibratome. The sections were counterstained with Hoechst, mounted onto glass slides, and secured under a coverslip with Vectashield Antifade Mounting Medium.

*Nissl staining.* Brain sections were dehydrated in a series of ethanol solutions (50%, 70%, 95%, and 99.8%), cleared in xylene and rehydrated. The sections were rinsed in tap water and stained with 0.13% (w/v) Cresyl violet solution (Cat. no. CS202101, Millipore) for 4 min, rinsed and dehydrated again as described above. The slices were washed in xylene and mounted using EuKitt.

*Western blot analysis.* Protein extracts were obtained from the thalami homogenized in ice-cold RIPA buffer. Protein concentrations were determined using Bio-Rad protein assay (Cat. no. 5000006, Bio-Rad Laboratories). Clarified protein homogenate (50 μg) was loaded on 10% SDS-polyacrylamide gels. Separated proteins were then transferred to Immun-Blot PVDF membranes (Cat. no. 1620177, Bio-Rad Laboratories), which were then blotted with anti-TCF7L2 and anti-β-actin (Cat. no. A3854, Sigma-Aldrich) antibodies. The staining was visualized with peroxidase substrate for enhanced chemiluminescence (ECL) and 200 μM coumaric acid. Images were captured using Amersham Imager 600 RGB (General Electric).

*RNA isolation.* *Tcf7l2*$^{-/-}$ and WT littermate mice were collected on E18.5, and *Cck*$^{Cre}$*:Tcf7l2*$^{fl/fl}$ and *Cck*$^{Cre}$*:Tcf7l2*$^{+/+}$ mice on P60. Their thalami together with the habenula (prosomere 2) were dissected-out. RNA was extracted using QIAzol (Cat. no. 79306, Qiagen) and the RNeasyMini Kit (Cat. no. 74106, Qiagen).

*RNAseq analysis.* The quality of RNA was verified in Bioanalyzer (Aligent). RNA samples were sequenced on the same run of Illumina HiSeq2500. The reads were aligned to the mouse genome mm10 assembly, from UCSC using HISAT (Kim D et al. 2015) and their counts were generated using HTSeq (Anders S et al. 2015). Raw read counts were normalized to gene length

per kilobase per million reads (RPKM). The genes with RPKM = 0 in at least one sample were discarded, along with genes with mean RPKM < 0.1. For the rest of the genes, fold-changes (FC = mean RPKMs of KO/WT) were calculated and two-tailed Student's t-test was performed. Genes with $\log_2(FC) > 0.5$ and $\log_2(FC) < -0.5$ and p-value < 0.05 were considered to be differentially expressed up- and downregulated genes (DEGs).

*Functional enrichment analysis.* Gene ontology (GO) enrichment for the DEGs was performed using an open access online tool GOrilla (http://cbl-gorilla.cs.technion.ac.il/). Two unranked lists of genes, one target (DEGs) and one universal (non-DEGs) were used, assuming a hypergeometric distribution of the unranked genes. As the universal set we used all the genes with expression measurements RPKM > 0.1 in all samples. GO-Term enrichments were tested with Fisher's exact test, and Bonferroni corrected $q$ values <0.05 were considered significant.

*Spatial expression of GO enriched genes.* The spatial localization of transcription factor and guidance/adhesion molecules DEGs was assessed by visual inspection and manual curation of the *in situ* hybridisation signals on E18.5 and P56 in the Allen Brain Atlas (ABA) (Allen Mouse Brain Atlas. 2004; Allen Developing Mouse Brain Atlas. 2008). The genes were then clustered into groups: thalamic; habenular, thalamo-habenular; boundary of prosomere 2; outside prosomere 2; non-specific (i.e. their expression was ubiquitous in the brain or no expression signal was observed in the atlas) and not available in ABA.

*Motif enrichment analysis in putative regulatory elements.* Nencki Genomics Database (NGD) v. 79_1 (Krystkowiak I et al. 2013) was used to map genes to their putative regulatory regions within ±10 Kb of the genomic DNA sequence that flanked the transcription start site. Human-mouse CNRs (conserved non-coding regions) (Bray N et al. 2003) were considered the putative

regulatory regions. In these regions, instances of all transcription factor binding sites (position weight matrices [PWMs]) that were available in NGD v79_1, representing 684 distinct transcription factors (Dabrowski M et al. 2015) were considered potential binding sites. As the universal set, we used all genes with both average expression measurements of RPKM ≥ 0.1 and at least one CNR. For Fisher's exact test, each instance of a motif was labelled with the names of its associated transcription factors. Fisher's test *p* values were Bonferroni corrected to obtained *q* values.

*In vitro slice electrophysiology*. Experiments were done in mice of both sexes on P21-23. 300 µm thick brain slices were cut (Ying SW and PA Goldstein 2005), recovered and recorded at 24°C in regular artificial cerebrospinal fluid (ACSF) equilibrated with 95/5% O2/CO2. Thalamocortical neurons in the ventrobasal complex were targeted for whole-cell patch-clamp recording with borosilicate glass electrodes (resistance 4-8 MΩ). Recordings were collected with a Multiclamp amplifier and Digidata 1550A digitizer and pClamp10.6 (Molecular Devices), and then sampled and filtered at 10 kHz. Analysis of action potentials was performed in Clampfit 10.6.

## Results

*Generation of mice with the complete and conditional knockouts of Tcf7l2*

To investigate the role of TCF7L2 in the prosomere 2 derivatives during development and in adult we used two different mice knockout models. The complete knockout of *Tcf7l2* (*Tcf7l2*$^{tm1a/tm1a}$, hereinafter referred to as *Tcf7l2*$^{-/-}$) was generated by an insertion of the tm1a(KOMP)Wtsi allele upstream of the critical 6$^{th}$ exon of the *Tcf7l2* gene (Supplementary Fig. 1A). *Tcf7l2*$^{tm1a}$ allele led to the production of truncated *Tcf7l2* mRNA and the lack of TCF7L2 protein, confirmed by immunostaining and Western blot (Supplementary Fig. 1B-C). *Tcf7l2*$^{-/-}$ mice die after birth. To create thalamus-specific postnatal knockout of *Tcf7l2* we first crossed *Tcf7l2*$^{+/tm1a}$ mice with transgenic animals that expressed flippase and then with mice that expressed CRE recombinase from the *Cck* promoter. The resulting *Cck*$^{Cre}$:*Tcf7l2*$^{fl/fl}$ mice had the 6$^{th}$ *Tcf7l2* exon removed perinatally in the thalamus. In adult *Cck*$^{Cre}$:*Tcf7l2*$^{fl/fl}$ animals TCF7L2 was absent in most thalamic nuclei, but was maintained in the habenula (Supplementary Fig. 1D-F).

*Normal neurogenesis but disrupted subregional anatomy in the embryonic thalamus and habenula*

The complete knockout of *Tcf7l2* did not cause any apparent defects in proliferation or neurogenesis in prosomere 2 at E12.5 (Supplementary Fig. 2). Transcription from the *Tcf7l2* locus was not abolished by *Tcf7l2* knockout in the postmitotic thalamus (Supplementary Fig. 3), confirming that the cells in this region were not generated in other parts of the neural tube.

To assess whether *Tcf7l2* knockout affected anatomical regionalisation in prosomere 2, we analysed the morphology of this region by Nissl staining of E18.5 brain sections (Fig. 1A-B). At that time, anatomical boundaries were well established in this area in WT mice. The boundaries between the prosomere 2 area and neighbouring structures, i.e., prethalamus and

pretectum, were not morphologically detected in knockout mice. Moreover the knockout thalami were underdeveloped and reduced in the radial dimension, resulting in an oval-like shape of this structure, and fused with the habenulae.

To investigate cell segregation and molecular boundary formation in prosomere 2, we analysed the spatial expression of markers that normally sharply delineate prosomere 2 and its subregions on E18.5. To identify prosomere 2, we stained brain sections with anti-TCF7L2 (WT mice) or anti-LacZ (knockout mice) antibodies. In control embryos, the thalamic area was separated from a characteristic, narrow strip of PAX6-expressing cells in the prethalamic subdomain at the rostroventral thalamic border (Fig. 1C). NKX2-2-positive area of rostral thalamic (rTh) region, which produce GABAergic interneurons (Evangelio M et al. 2018), created a sharp boundary with TCF7L2-high glutamatergic area of the thalamus (Fig. 1D). In *Tcf7l2* knockout embryos, both borders devoid of their characteristic sharpness, and some prethalamic and rTh cells invaded the glutamatergic thalamus. In WT embryos, the habenula was easily identified by POU4F1 staining (Quina LA *et al.* 2009), and the differences in cell densities allowed discernment of its lateral and medial parts (Fig. 1E). In knockout embryos, we observed extensive intermingling of POU4F1-positive cells into the neighbouring thalamic territories.

*Disrupted connectivity in prosomere 2*

To observe the formation of axonal connections in the forebrain in E18.5 *Tcf7l2*$^{-/-}$ embryos, we immunostained brain sections with an anti-L1CAM antibody, in addition to the aforementioned Nissl staining. These stainings revealed several impairments in connectivity in the diencephalon of *Tcf7l2*$^{-/-}$ embryos. The major habenular efferent tract, the fasciculus retroflexus (habenulo-interpeduncular tract), was virtually absent (Fig. 1B). The bundles of stria medullaris, which include afferent fibres from the basal forebrain and lateral hypothalamus to

the habenula, were disorganised and less compact (Fig. 1F). The fasciculation and arborisation of afferent retinal ganglion cell axons in the lateral geniculate nucleus and pregeniculate nucleus of the thalamus were also severely disturbed (Fig. 1F). The nerve fascicles that passed through the striatum, which include thalamocortical axons, were thinner and fewer in number (Fig. 1G). To test whether this resulted from the lack of thalamic projections, we traced these axons with DiI. None of the mutant embryos developed thalamocortical axons that would cross the striatum and invade the cortical subplate (Fig. 1H-I). In summary, TCF7L2 regulates the topography of thalamic and habenular circuits.

*Disrupted postmitotic patterning of the thalamus and habenula during embryogenesis and in adult*

Extensive and various anatomical impairments in prosomere 2 in *Tcf7l2*$^{-/-}$ embryos suggested a disruption of regional postmitotic patterning. To investigate whether the loss of *Tcf7l2* impaired the initial acquisition of postmitotic molecular identities in the thalamus and habenula, we first examined the expression of the *Gbx2* gene and POU4F1 protein during neurogenesis (E12.5). *Gbx2* and *Pou4f1* are the earliest markers of postmitotic neurons in the thalamus and habenula, respectively, and are critically involved in postmitotic differentiation in these regions (Bulfone A et al. 1993; Quina LA *et al.* 2009). Both *Gbx2* mRNA and POU4F1 were detected in the expected areas in both WT and *Tcf7l2*$^{-/-}$ embryos (Fig. 2A), demonstrating that TCF7L2 is not involved in the induction of their expression. We also noted that *Gbx2*-positive and POU4F1-positive areas expanded extensively into each other's territory, suggesting an early defect in thalamo-habenular boundary formation.

Next, to examine the effect of TCF7L2 deficiency on the thalamic and habenular molecular anatomy at the stage of postmitotic differentiation, we analysed the spatial pattern of marker gene expression. *Tcf7l2*$^{-/-}$ embryos exhibited a severe reduction of *Gbx2* expression in

the thalamus (Fig. 2B). *Gbx2* staining was still present in some periventricular cells, where the youngest neurons are located, but absent in the intermediate and superficial portions of the thalamus. The expression of *Prox1*, *Rora*, *Lef1,* and *Foxp2* was observed in many thalamic nuclei in WT embryos at this age but was virtually absent in the thalamic area in *Tcf7l2*$^{-/-}$ (Fig. 2B). In the habenula, *Tcf7l2* knockout significantly reduced the number of POU4F1-positive cells on E18.5 (Fig. 1E) and abolished the expression of *Etv1*, (Fig. 2C), and *Lef1* (Fig. 2B) in different habenular subregions, without affecting their expression in the pallium (*Etv1* in the cortex and *Lef1* in the dentate gyrus of the hippocampus). In contrast, in the GABAergic region of the rTh, where TCF7L2 is not present or low in the control condition, the expression of markers *Nkx2-2* and *Sox14* was preserved in *Tcf7l2* knockouts (Fig. 2D).

We then sought to determine whether the continuous presence of TCF7L2 is required to maintain post-developmental molecular patterning of the thalamus using adult *Cck*$^{Cre}$:*Tcf7l2*$^{fl/fl}$ mice. The gross anatomy of the thalamus was not visibly altered by the postnatal knockout of *Tcf7l2* in Nissl-stained sections, and the expression pattern of *Gbx2* and *Lef1* was unaltered in *Cck*$^{Cre}$:*Tcf7l2*$^{fl/fl}$ mice (Fig. 2E). However, the signal from *Rora* mRNAs was weaker in the medial thalamus, and *Prox1* expression markedly decreased in the thalamus but remained high in the hippocampus.

Concluding, TCF7L2 is continuously required to maintain a combinatorial network of prosomere 2-specific transcription factors during development and in adult.

*Disrupted prosomere 2-specific regulatory network during the development of axonal connections*

To gain an insight into the role of TCF7L2 in regulating prosomere 2 nucleogenesis and axon growth, we analysed global gene expression by RNA-seq in the thalamo-habenular domain in *Tcf7l2*$^{-/-}$ embryos. We identified 209 down-regulated and 137 upregulated genes

(Supplementary Fig. 4, Supplementary Table 3). Gene ontology (GO) term analysis (Supplementary Table 4) revealed an overrepresentation of transcription factor genes and genes that are involved in axon guidance, cell migration, cell adhesion, signal transducing activity and calcium ion binding.

To determine whether the differentially expressed genes are specific for prosomere 2, we inspected *in situ* hybridisation images of brain sections in the ABA. Approximately 85% of the tested genes that were downregulated were specific for the thalamus, habenula, or both (Fig. 3), such as *Epha4*, *Ntng1* (Netrin G1), and *Robo3*, which were shown to be important regulators of the guidance of thalamic or habenular efferent connections and the segregation of neurons in this region (Braisted JE et al. 2000; Dufour A et al. 2003; Lehigh KM et al. 2013; Belle M et al. 2014). In contrast, among the upregulated genes, only one of several dozen genes was prosomere 2-specific. These results implied that TCF7L2 controls the wiring of the thalamus and habenula during embryogenesis by regulating region-specific differentiation programs.

Because many transcription factor genes that were down-regulated in *Tcf7l2* knockout embryos (Fig. 2B-C and 3) are well known markers of thalamic or habenular nuclei (Nagalski A, L Puelles*, et al.* 2016), we hypothesed that TCF7L2 is a part of a transcription factor network that orchestrates morphological maturation of this area. To test this hypothesis we searched for overrepresented transcription factor regulatory motifs in putative regulatory elements of genes that were differentially expressed in prosomere 2 in *Tcf7l2*$^{-/-}$ embryos on E18.5. Out of 684 motifs analysed, a total of 81 motifs were over-represented in down-regulated genes (cluster 1), 229 motifs were over-represented in upregulated genes (cluster 2), and 556 motifs were over-represented in the complement of cluster 0 (all DEGs) (Supplementary Table 5). Such high numbers of over-represented motifs are characteristic of developmental and neural genes (Lee S et al. 2005; Dabrowski M et al. 2010). The TCF7L2 motif was highly ranked in all clusters. The motifs of GBX2, LEF1, POU4F1 and NR4A2 were also significantly overrepresented in

the complement of cluster 0. Together with strong activation of the *Gbx2*, *Pou4f1*, and *Nr4a2* promoters by the thalamus-specific isoform of TCF7L2 in the luciferase assay that was previously reported by our group (Nagalski A, L Puelles*, et al.* 2016), the present *in silico* analysis implied that TCF7L2 controls the expression of thalamic and habenular genes during embryogenesis directly and by maintaining a network of subregional transcription factors.

*Normal acquisition of glutamatergic identity but impairments in electrophysiological phenotype in thalamic neurons*

The loss of postmitotic subregional patterning in prosomere 2 could impair the acquisition or the maintenance of neurotransmitter identity in this region. Habenular and thalamic neurons in rodents (except GABAergic interneurons derived from rTh (Evangelio M *et al.* 2018)), are glutamatergic and express high levels of a vesicular glutamate transporter VGLUT2 (Fremeau RT et al. 2001; Herzog E et al. 2001). To determine whether TCF7L2 is involved in the adoption and of glutamatergic fate in the thalamus and habenula, we examined the expression patterns of *Vglut2* (*Slc17a6*) and *Gad67* (marker of GABAergic neurons) in the diencephalon in $Tcf7l2^{-/-}$ embryos and $Cck^{Cre}:Tcf7l2^{fl/fl}$ P60 adult mice. Both knockout strains exhibited a pattern of GABAergic and glutamatergic cell distribution that was similar to the WT condition, with predominant *Vglut2* expression in prosomere 2 (Fig. 4A and B). Thus, TCF7L2 is not involved in the specification of generic neurotransmitter identity in prosomere 2.

Using RNA-seq, we identified many 'excitability' genes that were specifically expressed in prosomere 2 and downregulated in $Tcf7l2^{-/-}$ embryos (Fig. 4C), such as thalamus-specific *Grik3* (ionotropic glutamate receptor) and *Slc6a4* (serotonin transporter) and habenula-specific *Kcng4* (Kv6.4 potassium voltage-gated channel) and *Chrnb4* (cholinergic receptor). Given that many of these types of genes are induced later in development, we sought to

determine the way in which the postnatal knockout of *Tcf7l2* influences their expression. We compared global gene expression profiles in the thalamus between *Cck*$^{Cre}$:*Tcf7l2*$^{tm1c/tm1c}$ and WT mice on P60 using RNA-seq. Of 326 genes that were differentially expressed, 176 were downregulated in knockout mice, and 150 were upregulated (Supplementary Fig. 4, Supplementary Table 6). The motif enrichment analysis of regulatory regions of DEGs in adult *Cck*$^{Cre}$:*Tcf7l2*$^{tm1c/tm1c}$ mice, in contrast to observations in *Tcf7l2*$^{-/-}$ embryos, showed substantially fewer overrepresented motifs (30, 6, and 110 in clusters 1, 2, and 0, respectively), and neither the TCF7L2 motif nor GBX2 or LEF1 were in this group (Supplementary Table 7). This suggests that TCF7L2 is a part of different regulatory networks at different developmental stages, and its role in direct gene expression regulation in the adult thalamus is less important. The GO analysis showed that the differentially expressed genes were significantly enriched with terms that clustered into groups of synaptic proteins, proteins that are involved in the regulation of membrane conductance, and components of signalling pathways (Supplementary Table 8, Fig. 4). We then examined spatial expression profiles of the identified genes in this cluster in the ABA. Approximately 45% of these genes were expressed specifically in the thalamus (Fig. 4), such as *Kcnc2* and *Cacna1g*, which encode subunits of Kv3.2 voltage-gated potassium channels and Cav3.1 voltage-gated calcium channels, respectively. Conversely, only a few of the upregulated excitability genes were thalamus-specific. Thus, postnatally, TCF7L2 regulates a battery of genes that shape electrophysiological identities of thalamic neurons.

*Severe impairments in excitability of thalamic neurons in adult mice*

To directly test electrophysiological properties of thalamic neurons, we used whole-cell patch-clamp recordings in *Cck*$^{Cre}$:*Tcf7l2*$^{fl/fl}$ mice by targeting thalamocortical neurons in the ventrobasal complex (VB). We first tested basic properties of VB neurons (i.e., resting potential, input resistance, and capacitance), which were similar in WT and knockout mice (Fig.

5A). We then examined whether the targeted neurons were able to evoke action potentials (APs; e.g., tonic, burst, and rebound burst modes) that are typical for thalamocortical cells. We used depolarizing current steps to evoke both sustained trains of APs (tonic) and burst firing at the beginning of a train (Fig. 5B, D). Rebound bursts were evoked by steps of hyperpolarizing current (Fig. 5C). Thalamic cells produced fewer APs in *Cck*$^{Cre}$*:Tcf7l2*$^{fl/fl}$ mice in both tonic and burst firing modes (Fig. 5E). Rebound bursts, which are crucial for the response of thalamocortical neurons to inhibitory input, were reduced (Fig. 5F, G). Most neurons from *Tcf7l2* knockout mice did not show any rebound bursts at the hyperpolarizing membrane potential (-65 mV; Fig. 5F). Hyperpolarizing steps that were applied at the resting membrane potential (~ -57 mV) evoked rebound burst spiking in VB neurons in *Cck*$^{Cre}$*:Tcf7l2*$^{fl/fl}$ mice, but the frequency of spikes was approximately two-times lower compared with WT mice (Fig. 5G). These dramatic impairments in excitability and firing modes demonstrated that TCF7L2 is required for the establishment of unique firing patterns in thalamocortical neurons.

## Discussion

Little is understood about the way in which the lengthy process of postmitotic differentiation is regulated in the vertebrate brain. We sought to reveal mechanisms that govern development of the thalamus and habenula, which both derive from the prosomere 2 progenitor domain and are implicated in mental disorders. The present study identified TCF7L2 as a master selector of prosomere 2 neurons that functions at several developmental stages. TCF7L2 controls the maintenance of thalamic and habenular postmitotic patterning and has stage-specific functions in the establishment of axonal connections in these regions and the development of terminal electrophysiological features in thalamic neurons.

*TCF7L2 controls the prosomere 2-specific network of transcription factors to regulate the formation of prosomere 2 nuclei and axonal connections*

TCF7L2 is the only developmentally regulated transcription factor that is expressed throughout prosomere 2 (Nagalski A, K Kozinski, et al. 2016). The expression of both pan-thalamic *Gbx2* and pan-habenular *Pou4f1* was observed in *Tcf7l2*$^{-/-}$ embryos on E12.5 but was reduced on E18.5 and was detected only where the youngest thalamic and habenular neurons were present. Subregional patterning with transcription factor genes that have a spatially limited pattern of expression in the thalamus or habenula was abolished in *Tcf7l2*$^{-/-}$ embryos. Among these markers were sub-thalamic *Foxp2* and *Rora* and sub-habenular *Nr4a2*. These findings are consistent with our previous results that showed that TCF7L2 regulates promoters of *Rora*, *Foxp2*, *Nr4a2*, and *Etv1*, as well as *Gbx2* and *Pou4f1* (Nagalski A, L Puelles*, et al.* 2016). *Foxp2* and *Rora* were also downregulated in *Gbx2*$^{-/-}$ embryos (Mallika C *et al.* 2015), whereas the expression of *Nr4a2* and *Etv1* decreased in *Pou4f1*$^{-/-}$ embryos, and *Nr4a2* knockout affected the expression of *Etv1* (Quina LA *et al.* 2009). These expression patterns imply a hierarchical pattern of regulation of the expression of regional and subregional

prosomere 2 transcription factors and suggest that TCF7L2 plays a master role in the maintenance of regional identities in postmitotic prosomere 2.

Similarities between phenotypes in *Gbx2*$^{-/-}$ and *Tcf7l2*$^{-/-}$ mice suggest that at least some of the functions of TCF7L2 in development of the thalamus are mediated by GBX2. These similarities in *Tcf7l2*$^{-/-}$ and *Gbx2*$^{-/-}$ embryos included anatomical impairments in the thalamus, such as elongated shape of the thalamus, no parcellation of the thalamus into discrete nuclei, impairments in cell sorting at thalamic boundaries, and the absence of thalamocortical projections (Chen L *et al.* 2009; Chatterjee M *et al.* 2012). Decreases in the expression of genes that encode prosomere 2-specific cell adhesion molecules (e.g., Cadherins 6 and 8 and Contactin 6) and axon-navigating molecules (e.g., Netrin G1 and Ephrin receptor 4), which we observed in the present study, may underlie anatomical defects in *Tcf7l2*$^{-/-}$ mice. The expression of *Cdh6* and *Ntng1* was also disrupted in the thalamus in *Gbx2* mutant embryos (Chen L *et al.* 2009; Mallika C *et al.* 2015), suggesting that these genes might be indirectly regulated by TCF7L2. FOXP2 and RORA could also contribute to the defects that were observed in *Tcf7l2* and *Gbx2* knockout mice, because some subregional impairments in the growth and sorting of thalamocortical connections were reported in *Foxp2* (Ebisu H *et al.* 2016) and *Rora* (Vitalis T *et al.* 2017) knockout mice. Lee at al. recently reported that TCF7L2 regulates the pathfinding of thalamocortical axons in a GBX2-independent manner, in which essentially normal *Gbx2* expression was observed in *Tcf7l2*$^{-/-}$ mice on E12.5 (Lee M *et al.* 2017). We speculate that GBX2 can contribute to this phenotype because its expression was not maintained in the thalamus in *Tcf7l2*$^{-/-}$ mice at later embryonic stages when thalamocortical axons navigate through the ventral telencephalon

Similarities also exist between *Pou4f1*$^{-/-}$ and *Tcf7l2*$^{-/-}$ mice with regard to alterations of gene expression profiles. In both cases, the habenular axon guidance genes *Rgma* and *Epha8* and habenular cholinergic receptor gene *Chrnb4* were downregulated, in addition to the

aforementioned *Nr4a2* and *Etv1* habenular patterning genes (Quina LA *et al.* 2009). However, anatomical impairments in the habenula were much more severe in *Tcf7l2* mutant embryos. For example, habenulo-interpeduncular tracts, which were present in *Pou4f1* and *Nr4a2* knockout embryos (Quina LA *et al.* 2009; Serrano-Saiz E *et al.* 2018), were completely missing in *Tcf7l2*$^{-/-}$ embryos. This indicates that TCF7L2 plays critical roles in postmitotic development of the habenula independently of POU4F1.

In conclusion, downstream developmental programs in prosomere 2 are likely regulated by TCF7L2 both directly and indirectly via regional and subregional transcription factors. This possibility is corroborated by overrepresentations of GBX2, POU4F1, and NR4A2 binding motifs and the TCF7L2 motif in regulatory elements of genes that were differentially expressed in prosomere 2 in *Tcf7l2*$^{-/-}$ embryos. Further research is required to determine the way in which TCF7L2 cooperates with regional and subregional transcriptions factors to control developmental gene expression in thalamic and habenular nuclei.

*TCF7L2 controls the adoption of characteristic excitability profiles in the thalamus*

Excitability and synaptic transmission parameters are specific to different classes of neurons and together ensure the proper functioning of neural circuits in the brain. Many genes that were downregulated in mice with the total or post-developmental knockout of *Tcf7l2* encode either thalamus- or habenula-specific neurotransmitter receptors or transporters, voltage-gated ion channels, and other proteins that are involved in neural signal transmission, which is consistent with our previous *in silico* predictions (Wisniewska MB *et al.* 2012).

Among the genes that were downregulated in *Tcf7l2*$^{-/-}$ embryos, we identified the habenular genes *Chrnb4* and *Slc5a7*, which encode the choline transporter and acetylcholine receptor subunit, respectively, and the thalamus-specific serotonin transporter gene *Slc6a4*, which is transiently expressed during development (Lebrand C et al. 1998) and is involved in

the development of thalamocortical connectivity (Persico AM et al. 2001; Bonnin A et al. 2007). Notably, components of cholinergic signalling in the habenula are involved in depressive behaviour (Han S et al. 2017), whereas variants of *SLC6A4* are associated with autism spectrum disorder (Coutinho AM et al. 2004). Moreover, the transient pharmacological inhibition of *Slc6a4* during early development produced abnormal emotional behaviours in adult mice (Ansorge MS et al. 2004). This suggests that electrophysiological dysfunctions of the thalamus and habenula, which could result from impairments in TCF7L2 activity during development, may underlie some pathologies in psychiatric disorders.

In adult mice with the postnatal knockout of *Tcf7l2*, many excitability genes were downregulated in the thalamus, including pan-thalamic *Cacna1g* and *Kcnc2*, which encode the T-type voltage-gated calcium channel and Kv3.2 potassium channel, respectively. Our group previously showed that *Cacna1g* is a direct target of LEF1/TCF and β-catenin in the adult thalamus (Wisniewska MB et al. 2010). Functional experiments showed that both burst and tonic firing modes were significantly reduced in knockout thalamocortical neurons. These changes in thalamic neuron excitability reflect the aforementioned changes in the expression of multiple ion channels. The downregulation of *Cacna1g* and *Kcnc2* likely contributed to this phenotype. In thalamocortical neurons, *Cacna1g* knockout resulted in the absence of burst firing (Kim D et al. 2001), whereas Kv3.2 channel inhibition suppressed the firing rate in tonic mode (Kasten MR et al. 2007), similar to our observations in *Tcf7l2* knockout mice. These results indicate that TCF7L2 regulates the expression of ion channels that are crucial for normal electrophysiological activities of thalamocortical relay neurons, which lose their proper tonic and burst firing patterns in the absence of TCF7L2.

*TCF7L2 is a terminal selector of cell fates in prosomere 2*

TCF7L2 meets the criteria of a thalamic terminal selector in prosomere 2. Its expression is induced during neurogenesis and maintained in prosomere 2 neurons throughout life (Nagalski A *et al.* 2013). Additionally, TCF7L2 binding motifs are overrepresented in prosomere 2-specific genes (Nagalski A, K Kozinski*, et al.* 2016). The present study showed that TCF7L2 activity is required for electrophysiological maturation of the thalamus. Only a few examples of such regulators that operate in the vertebrate brain have been reported (Hobert O 2016). Most of the known selectors are specific to different classes of aminergic neurons, such as NR4A2 and PITX in midbrain dopaminergic neurons (Kadkhodaei B et al. 2009), ETV1 in dopaminergic neurons in the olfactory bulbs (Cave JW et al. 2010), ISL1 and LHX7 in forebrain cholinergic neurons (Lopes R et al. 2012), and PET1 in serotonergic neurons (Liu C et al. 2010). POU4F1 was recently identified as a selector of glutamatergic neurons in the medial habenula, where it maintains expression of the glutamate transporter gene *Vglut1* (*Slc17a7*) (Serrano-Saiz E *et al.* 2018). Unlike the other identified vertebrate selectors, which are neuron subtype-specific, TCF7L2 is a regional selector that controls the adoption of different subregional cell fates during embryogenesis by regulating a hierarchical network of regional transcription factors. Unlike other terminal selectors, TCF7L2 does not determine the generic neurotransmitter identity of neurons, which in the thalamus depends on *Vglut2* (*Slc17a6*). This indicates that in vertebrates, the development of neurotransmitter identity and electrophysiological phenotype can be uncoupled. This may be related to timely separation of the initiation of neurotransmitter identity and postnatal electrophysiological maturation. More research is needed to determine whether this is a rule or an exception in the development of glutamatergic neurons in vertebrates.

*Conclusion*

TCF7L2 functions as a regional terminal selector in the vertebrate brain. It regulates subregional routines of postmitotic development in the thalamus and habenula by orchestrating a hierarchical network of transcription factors. It plays a dual role in morphological and electrophysiological maturation in these regions at different developmental stages. The regulation of thalamic terminal selection by TCF7L2 provides evidence that the establishment of neurotransmitter identity and specific excitability patterns can be uncoupled in vertebrates. Considering that *Tcf7l2* has been associated with mental disorders, our findings provide insights into the aetiology of thalamic and habenular dysfunctions that are observed in these disorders.

**Funding**

This work was supported by the Polish National Science Centre (grant number 2011/03/B/NZ3/04480, 2015/19/B/NZ3/02949 to MBW). AN and KK were additionally supported by the Polish National Science Centre (grant number 2015/19/B/NZ4/03571), JLF and AT were supported and by the Seneca Foundation, Comunidad de Murcia (grant number 19904/GERM/1 to JLF).

**Acknowledgements**

We thank the Genomics Core Facility at the Centre of Genomic Regulation (CRG, Spain) for providing next-generation sequencing services. We gratefully acknowledge M. Irimia from CRG, K. Misztal from the International Institute of Molecular and Cell Biology (Poland), K. Debski from the Nencki Institute of Experimental Biology (Poland), and L. Szewczyk in our Laboratory for help with the RNA-seq analysis. We thank K. Brzozowska in our Laboratory for the initial management of the mice colony. A part of genotyping was performed at the Laboratory of Animal Models facility at the Nencki Institute of Experimental Biology.

**Data availability**

The RNA-seq raw FASTQ files are in the process of uploading at the EMBL-EBI data repository - ArrayExpress. The EMAT number will be provided as soon as the datasets are accepted.

**Competing interests**

No competing interests declared.

## References


2004. Allen Institute for Brain Science. Allen Mouse Brain Atlas. Available from: https://mouse.brain-map.org.

2008. Allen Institute for Brain Science. Allen Developing Mouse Brain Atlas. Available from: http://developingmouse.brain-map.org.

2011. Allen Institute for Brain Science. Allen Brain Connectivity Atlas. Characterisation of Cck-IRES-Cre transgene. Available from: http://connectivity.brain-map.org/transgenic/imageseries/list/1.html?gene_term=Cck-IRES-Cre.

Anders S, Pyl PT, Huber W. 2015. HTSeq--a Python framework to work with high-throughput sequencing data. Bioinformatics. 31:166-169.

Ansorge MS, Zhou M, Lira A, Hen R, Gingrich JA. 2004. Early-life blockade of the 5-HT transporter alters emotional behavior in adult mice. Science. 306:879-881.

Antón-Bolaños N, Espinosa A, López-Bendito G. 2018. Developmental interactions between thalamus and cortex: a true love reciprocal story. Curr Opin Neurobiol. 52:33-41.

Belle M, Godefroy D, Dominici C, Heitz-Marchaland C, Zelina P, Hellal F, Bradke F, Chédotal A. 2014. A simple method for 3D analysis of immunolabeled axonal tracts in a transparent nervous system. Cell Rep. 9:1191-1201.

Benekareddy M, Stachniak TJ, Bruns A, Knoflach F, von Kienlin M, Künnecke B, Ghosh A. 2018. Identification of a Corticohabenular Circuit Regulating Socially Directed Behavior. Biol Psychiatry. 83:607-617.

Beretta CA, Dross N, Bankhead P, Carl M. 2013. The ventral habenulae of zebrafish develop in prosomere 2 dependent on Tcf7l2 function. Neural Dev. 8:19.

Bonnin A, Torii M, Wang L, Rakic P, Levitt P. 2007. Serotonin modulates the response of embryonic thalamocortical axons to netrin-1. Nat Neurosci. 10:588-597.

Braisted JE, Catalano SM, Stimac R, Kennedy TE, Tessier-Lavigne M, Shatz CJ, O'Leary DD. 2000. Netrin-1 promotes thalamic axon growth and is required for proper development of the thalamocortical projection. J Neurosci. 20:5792-5801.

Bray N, Dubchak I, Pachter L. 2003. AVID: A global alignment program. Genome Res. 13:97-102.

Bulfone A, Puelles L, Porteus MH, Frohman MA, Martin GR, Rubenstein JL. 1993. Spatially restricted expression of Dlx-1, Dlx-2 (Tes-1), Gbx-2, and Wnt-3 in the embryonic day 12.5 mouse forebrain defines potential transverse and longitudinal segmental boundaries. J Neurosci. 13:3155-3172.

Cadigan KM, Waterman ML. 2012. TCF/LEFs and Wnt signaling in the nucleus. Cold Spring Harb Perspect Biol. 4.

Cave JW, Akiba Y, Banerjee K, Bhosle S, Berlin R, Baker H. 2010. Differential regulation of dopaminergic gene expression by Er81. J Neurosci. 30:4717-4724.

Chatterjee M, Guo Q, Weber S, Scholpp S, Li JY. 2014. Pax6 regulates the formation of the habenular nuclei by controlling the temporospatial expression of Shh in the diencephalon in vertebrates. BMC Biol. 12:13.

Chatterjee M, Li K, Chen L, Maisano X, Guo Q, Gan L, Li JY. 2012. Gbx2 regulates thalamocortical axon guidance by modifying the LIM and Robo codes. Development. 139:4633-4643.

Chen L, Guo Q, Li JY. 2009. Transcription factor Gbx2 acts cell-nonautonomously to regulate the formation of lineage-restriction boundaries of the thalamus. Development. 136:1317-1326.
Coutinho AM, Oliveira G, Morgadinho T, Fesel C, Macedo TR, Bento C, Marques C, Ataíde A, Miguel T, Borges L, Vicente AM. 2004. Variants of the serotonin transporter gene (SLC6A4) significantly contribute to hyperserotonemia in autism. Mol Psychiatry. 9:264-271.
Dabrowski M, Dojer N, Krystkowiak I, Kaminska B, Wilczynski B. 2015. Optimally choosing PWM motif databases and sequence scanning approaches based on ChIP-seq data. BMC Bioinformatics. 16:140.
Dabrowski M, Dojer N, Zawadzka M, Mieczkowski J, Kaminska B. 2010. Comparative analysis of cis-regulation following stroke and seizures in subspaces of conserved eigensystems. BMC Syst Biol. 4:86.
Dufour A, Seibt J, Passante L, Depaepe V, Ciossek T, Frisén J, Kullander K, Flanagan JG, Polleux F, Vanderhaeghen P. 2003. Area specificity and topography of thalamocortical projections are controlled by ephrin/Eph genes. Neuron. 39:453-465.
Ebisu H, Iwai-Takekoshi L, Fujita-Jimbo E, Momoi T, Kawasaki H. 2016. Foxp2 Regulates Identities and Projection Patterns of Thalamic Nuclei During Development. Cereb Cortex.
Evangelio M, García-Amado M, Clascá F. 2018. Thalamocortical Projection Neuron and Interneuron Numbers in the Visual Thalamic Nuclei of the Adult C57BL/6 Mouse. Front Neuroanat. 12:27.
Fakhoury M. 2017. The habenula in psychiatric disorders: More than three decades of translational investigation. Neurosci Biobehav Rev. 83:721-735.
Farley FW, Soriano P, Steffen LS, Dymecki SM. 2000. Widespread recombinase expression using FLPeR (flipper) mice. Genesis. 28:106-110.
Fedtsova NG, Turner EE. 1995. Brn-3.0 expression identifies early post-mitotic CNS neurons and sensory neural precursors. Mech Dev. 53:291-304.
Ferran JL, Ayad A, Merchán P, Morales- Delgado N, Sánchez-Arrones L, Alonso A, Sandoval JE, Bardet SM, Corral-San-Miguel R, Sánchez-Guardado LÓ, Hidalgo-Sánchez M, Martínez-de-la-Torre M, Puelles L. 2015. Exploring Brain Genoarchitecture by Single and Double Chromogenic In Situ Hybridization (ISH) and Immunohistochemistry (IHC) in Whole-Mount Embryos. In. In Situ Hybridization Methods 1 ed. Humana Press p 61-82.
Ferran JL, Ayad A, Merchán P, Morales- Delgado N, Sánchez-Arrones L, Alonso A, Sandoval JE, Bardet SM, Corral-San-Miguel R, Sánchez-Guardado LÓ, Hidalgo-Sánchez M, Martínez-de-la-Torre M, Puelles L. 2015. Exploring Brain Genoarchitecture by Single and Double Chromogenic In Situ Hybridization (ISH) and Immunohistochemistry (IHC) on Cryostat, Paraffin, or Floating Sections. In. In Situ Hybridization Methods 1 ed. Humana Press p 83-107.
Fremeau RT, Troyer MD, Pahner I, Nygaard GO, Tran CH, Reimer RJ, Bellocchio EE, Fortin D, Storm-Mathisen J, Edwards RH. 2001. The expression of vesicular glutamate transporters defines two classes of excitatory synapse. Neuron. 31:247-260.
Gezelius H, Lopez-Bendito G. 2017. Thalamic neuronal specification and early circuit formation. Dev Neurobiol. 77:830-843.
Gezelius H, Moreno-Juan V, Mezzera C, Thakurela S, Rodríguez-Malmierca LM, Pistolic J, Benes V, Tiwari VK, López-Bendito G. 2017. Genetic Labeling of Nuclei-Specific Thalamocortical Neurons Reveals Putative Sensory-Modality Specific Genes. Cereb Cortex. 27:5054-5069.

Han S, Yang SH, Kim JY, Mo S, Yang E, Song KM, Ham BJ, Mechawar N, Turecki G, Lee HW, Kim H. 2017. Down-regulation of cholinergic signaling in the habenula induces anhedonia-like behavior. Sci Rep. 7:900.
Herzog E, Bellenchi GC, Gras C, Bernard V, Ravassard P, Bedet C, Gasnier B, Giros B, El Mestikawy S. 2001. The existence of a second vesicular glutamate transporter specifies subpopulations of glutamatergic neurons. J Neurosci. 21:RC181.
Hevner RF, Miyashita-Lin E, Rubenstein JL. 2002. Cortical and thalamic axon pathfinding defects in Tbr1, Gbx2, and Pax6 mutant mice: evidence that cortical and thalamic axons interact and guide each other. J Comp Neurol. 447:8-17.
Hikosaka O. 2010. The habenula: from stress evasion to value-based decision-making. Nat Rev Neurosci. 11:503-513.
Hikosaka O, Sesack SR, Lecourtier L, Shepard PD. 2008. Habenula: crossroad between the basal ganglia and the limbic system. J Neurosci. 28:11825-11829.
Hobert O. 2016. Terminal Selectors of Neuronal Identity. Curr Top Dev Biol. 116:455-475.
Husken U, Stickney HL, Gestri G, Bianco IH, Faro A, Young RM, Roussigne M, Hawkins TA, Beretta CA, Brinkmann I, Paolini A, Jacinto R, Albadri S, Dreosti E, Tsalavouta M, Schwarz Q, Cavodeassi F, Barth AK, Wen L, Zhang B, Blader P, Yaksi E, Poggi L, Zigman M, Lin S, Wilson SW, Carl M. 2014. Tcf7l2 is required for left-right asymmetric differentiation of habenular neurons. Curr Biol. 24:2217-2227.
Kadkhodaei B, Ito T, Joodmardi E, Mattsson B, Rouillard C, Carta M, Muramatsu S, Sumi-Ichinose C, Nomura T, Metzger D, Chambon P, Lindqvist E, Larsson NG, Olson L, Björklund A, Ichinose H, Perlmann T. 2009. Nurr1 is required for maintenance of maturing and adult midbrain dopamine neurons. J Neurosci. 29:15923-15932.
Kasten MR, Rudy B, Anderson MP. 2007. Differential regulation of action potential firing in adult murine thalamocortical neurons by Kv3.2, Kv1, and SK potassium and N-type calcium channels. J Physiol. 584:565-582.
Kim D, Langmead B, Salzberg SL. 2015. HISAT: a fast spliced aligner with low memory requirements. Nat Methods. 12:357-360.
Kim D, Song I, Keum S, Lee T, Jeong MJ, Kim SS, McEnery MW, Shin HS. 2001. Lack of the burst firing of thalamocortical relay neurons and resistance to absence seizures in mice lacking alpha(1G) T-type Ca(2+) channels. Neuron. 31:35-45.
Kobayashi Y, Sano Y, Vannoni E, Goto H, Suzuki H, Oba A, Kawasaki H, Kanba S, Lipp HP, Murphy NP, Wolfer DP, Itohara S. 2013. Genetic dissection of medial habenula-interpeduncular nucleus pathway function in mice. Front Behav Neurosci. 7:17.
Krystkowiak I, Lenart J, Debski K, Kuterba P, Petas M, Kaminska B, Dabrowski M. 2013. Nencki Genomics Database--Ensembl funcgen enhanced with intersections, user data and genome-wide TFBS motifs. Database (Oxford). 2013:bat069.
Lebrand C, Cases O, Wehrlé R, Blakely RD, Edwards RH, Gaspar P. 1998. Transient developmental expression of monoamine transporters in the rodent forebrain. J Comp Neurol. 401:506-524.
Lee M, Yoon J, Song H, Lee B, Lam DT, Baek K, Clevers H, Jeong Y. 2017. Tcf7l2 plays crucial roles in forebrain development through regulation of thalamic and habenular neuron identity and connectivity. Dev Biol. 424:62-76.

Lee S, Kohane I, Kasif S. 2005. Genes involved in complex adaptive processes tend to have highly conserved upstream regions in mammalian genomes. BMC Genomics. 6:168.
Lehigh KM, Leonard CE, Baranoski J, Donoghue MJ. 2013. Parcellation of the thalamus into distinct nuclei reflects EphA expression and function. Gene Expr Patterns. 13:454-463.
Li K, Zhang J, Li JY. 2012. Gbx2 plays an essential but transient role in the formation of thalamic nuclei. PLoS One. 7:e47111.
Lien AD, Scanziani M. 2018. Cortical direction selectivity emerges at convergence of thalamic synapses. Nature. 558:80-86.
Liu C, Maejima T, Wyler SC, Casadesus G, Herlitze S, Deneris ES. 2010. Pet-1 is required across different stages of life to regulate serotonergic function. Nat Neurosci. 13:1190-1198.
Lopes R, Verhey van Wijk N, Neves G, Pachnis V. 2012. Transcription factor LIM homeobox 7 (Lhx7) maintains subtype identity of cholinergic interneurons in the mammalian striatum. Proc Natl Acad Sci U S A. 109:3119-3124.
Mallika C, Guo Q, Li JY. 2015. Gbx2 is essential for maintaining thalamic neuron identity and repressing habenular characters in the developing thalamus. Dev Biol. 407:26-39.
Miyashita-Lin EM, Hevner R, Wassarman KM, Martinez S, Rubenstein JL. 1999. Early neocortical regionalization in the absence of thalamic innervation. Science. 285:906-909.
Nagalski A, Irimia M, Szewczyk L, Ferran JL, Misztal K, Kuznicki J, Wisniewska MB. 2013. Postnatal isoform switch and protein localization of LEF1 and TCF7L2 transcription factors in cortical, thalamic, and mesencephalic regions of the adult mouse brain. Brain Struct Funct. 218:1531-1549.
Nagalski A, Kozinski K, Wisniewska MB. 2016. Metabolic pathways in the periphery and brain: Contribution to mental disorders? Int J Biochem Cell Biol. 80:19-30.
Nagalski A, Puelles L, Dabrowski M, Wegierski T, Kuznicki J, Wisniewska MB. 2016. Molecular anatomy of the thalamic complex and the underlying transcription factors. Brain Struct Funct. 221:2493-2510.
Pergola G, Selvaggi P, Trizio S, Bertolino A, Blasi G. 2015. The role of the thalamus in schizophrenia from a neuroimaging perspective. Neurosci Biobehav Rev. 54:57-75.
Persico AM, Mengual E, Moessner R, Hall FS, Revay RS, Sora I, Arellano J, DeFelipe J, Gimenez-Amaya JM, Conciatori M, Marino R, Baldi A, Cabib S, Pascucci T, Uhl GR, Murphy DL, Lesch KP, Keller F, Hall SF. 2001. Barrel pattern formation requires serotonin uptake by thalamocortical afferents, and not vesicular monoamine release. J Neurosci. 21:6862-6873.
Price DJ, Clegg J, Duocastella XO, Willshaw D, Pratt T. 2012. The importance of combinatorial gene expression in early Mammalian thalamic patterning and thalamocortical axonal guidance. Front Neurosci. 6:37.
Puelles L, Morales-Delgado N, Merchán P, Castro-Robles B, Martínez-de-la-Torre M, Díaz C, Ferran JL. 2016. Radial and tangential migration of telencephalic somatostatin neurons originated from the mouse diagonal area. Brain Struct Funct. 221:3027-3065.
Quina LA, Wang S, Ng L, Turner EE. 2009. Brn3a and Nurr1 mediate a gene regulatory pathway for habenula development. J Neurosci. 29:14309-14322.
Ribary U. 2005. Dynamics of thalamo-cortical network oscillations and human perception. Prog Brain Res. 150:127-142.
Scholpp S, Lumsden A. 2010. Building a bridal chamber: development of the thalamus. Trends Neurosci. 33:373-380.

Serrano-Saiz E, Leyva-Díaz E, De La Cruz E, Hobert O. 2018. BRN3-type POU Homeobox Genes Maintain the Identity of Mature Postmitotic Neurons in Nematodes and Mice. Curr Biol. 28:2813-2823.e2812.
Sherman SM. 2017. Functioning of Circuits Connecting Thalamus and Cortex. Compr Physiol. 7:713-739.
Shimogori T, Lee DA, Miranda-Angulo A, Yang Y, Wang H, Jiang L, Yoshida AC, Kataoka A, Mashiko H, Avetisyan M, Qi L, Qian J, Blackshaw S. 2010. A genomic atlas of mouse hypothalamic development. Nat Neurosci. 13:767-775.
Skarnes WC, Rosen B, West AP, Koutsourakis M, Bushell W, Iyer V, Mujica AO, Thomas M, Harrow J, Cox T, Jackson D, Severin J, Biggs P, Fu J, Nefedov M, de Jong PJ, Stewart AF, Bradley A. 2011. A conditional knockout resource for the genome-wide study of mouse gene function. Nature. 474:337-342.
Suzuki-Hirano A, Ogawa M, Kataoka A, Yoshida AC, Itoh D, Ueno M, Blackshaw S, Shimogori T. 2011. Dynamic spatiotemporal gene expression in embryonic mouse thalamus. J Comp Neurol. 519:528-543.
Taniguchi H, He M, Wu P, Kim S, Paik R, Sugino K, Kvitsiani D, Kvitsani D, Fu Y, Lu J, Lin Y, Miyoshi G, Shima Y, Fishell G, Nelson SB, Huang ZJ. 2011. A resource of Cre driver lines for genetic targeting of GABAergic neurons in cerebral cortex. Neuron. 71:995-1013.
Vitalis T, Dauphinot L, Gressens P, Potier MC, Mariani J, Gaspar P. 2017. RORα Coordinates Thalamic and Cortical Maturation to Instruct Barrel Cortex Development. Cereb Cortex.1-14.
Vue TY, Bluske K, Alishahi A, Yang LL, Koyano-Nakagawa N, Novitch B, Nakagawa Y. 2009. Sonic hedgehog signaling controls thalamic progenitor identity and nuclei specification in mice. J Neurosci. 29:4484-4497.
Walther C, Gruss P. 1991. Pax-6, a murine paired box gene, is expressed in the developing CNS. Development. 113:1435-1449.
Wisniewska MB, Misztal K, Michowski W, Szczot M, Purta E, Lesniak W, Klejman ME, Dabrowski M, Filipkowski RK, Nagalski A, Mozrzymas JW, Kuznicki J. 2010. LEF1/beta-catenin complex regulates transcription of the Cav3.1 calcium channel gene (Cacna1g) in thalamic neurons of the adult brain. J Neurosci. 30:4957-4969.
Wisniewska MB, Nagalski A, Dabrowski M, Misztal K, Kuznicki J. 2012. Novel β-catenin target genes identified in thalamic neurons encode modulators of neuronal excitability. BMC Genomics. 13:635.
Ying SW, Goldstein PA. 2005. Propofol suppresses synaptic responsiveness of somatosensory relay neurons to excitatory input by potentiating GABA(A) receptor chloride channels. Mol Pain. 1:2.
Yuge K, Kataoka A, Yoshida AC, Itoh D, Aggarwal M, Mori S, Blackshaw S, Shimogori T. 2011. Region-specific gene expression in early postnatal mouse thalamus. J Comp Neurol. 519:544-561.

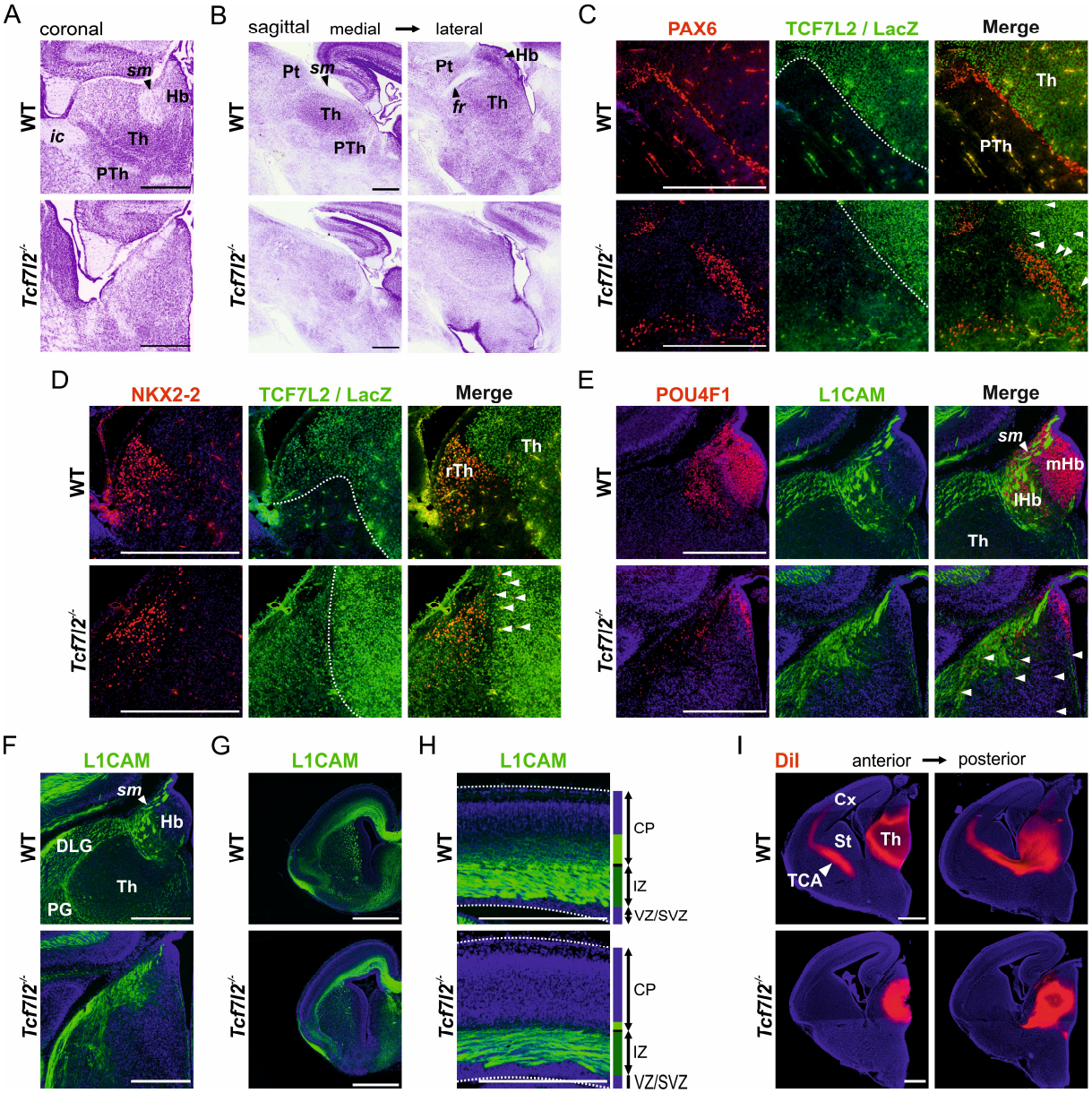


**Figure 1. TCF7L2 is necessary for the development of anatomical borders and axonal connectivity of the thalamus and habenula.** Nissl staining of coronal brain sections on P0 **(A)** and sagittal brain sections on E18.5 **(B)**. In *Tcf7l2*$^{-/-}$ embryos the shape of the thalamo-habenular region is changed and the anatomical boundaries are not visible. Immunofluorescent staining of TCF7L2 (in wildtype) or LacZ (in *Tcf7l2*$^{-/-}$) and PAX6 **(C)** or NKX2-2 **(D)** in coronal brain sections. PAX6-positive and NKX2-2-positive cells (marked with white triangles) abnormally invade the thalamus in *Tcf7l2*$^{-/-}$ embryos. **(E)** Immunofluorescent staining of the habenular marker POU4F1 and axonal marker L1CAM in coronal brain sections. The number of POU4F1-

positive cells is reduced in the habenular region in *Tcf7l2*$^{-/-}$ embryos. The remaining POU4F1-positive cells either accumulate in the subventricular region of the habenula or spread into the thalamic area (marked with white triangles), which is not separated from the habenula by axon fascicles. Immunofluorescent staining of the axonal marker L1CAM in thalamo-habenular **(F),** striatal (**G**) and cortical **(H)** regions. Axons in thalamic and habenular areas, including the *stria medullaris*, are disorganised, there are fewer fascicles in the striatum, and fewer axons invade the cortical plate in *Tcf7l2*$^{-/-}$ embryos. **(I)** DiI tracing of thalamocortical tracts. There is little to no thalamocortical axon growth in *Tcf7l2*$^{-/-}$ embryos. Cx, cortex; CP, cortical plate; DLG, dorsal lateral geniculate nucleus; Hb, habenula; lHb, lateral habenula; mHb, medial habenula; IZ, intermediate zone; ic, internal capsule; TCA, thalamocortical axons; Th, thalamus; PG, pregeniculate nucleus; Pt, pretectum; PTh, prethalamus; rTh, rostral thalamus; sm, stria medullaris; St, striatum; VZ/SVZ, ventricular/subventricular zone. Scale is 0.5 mm.

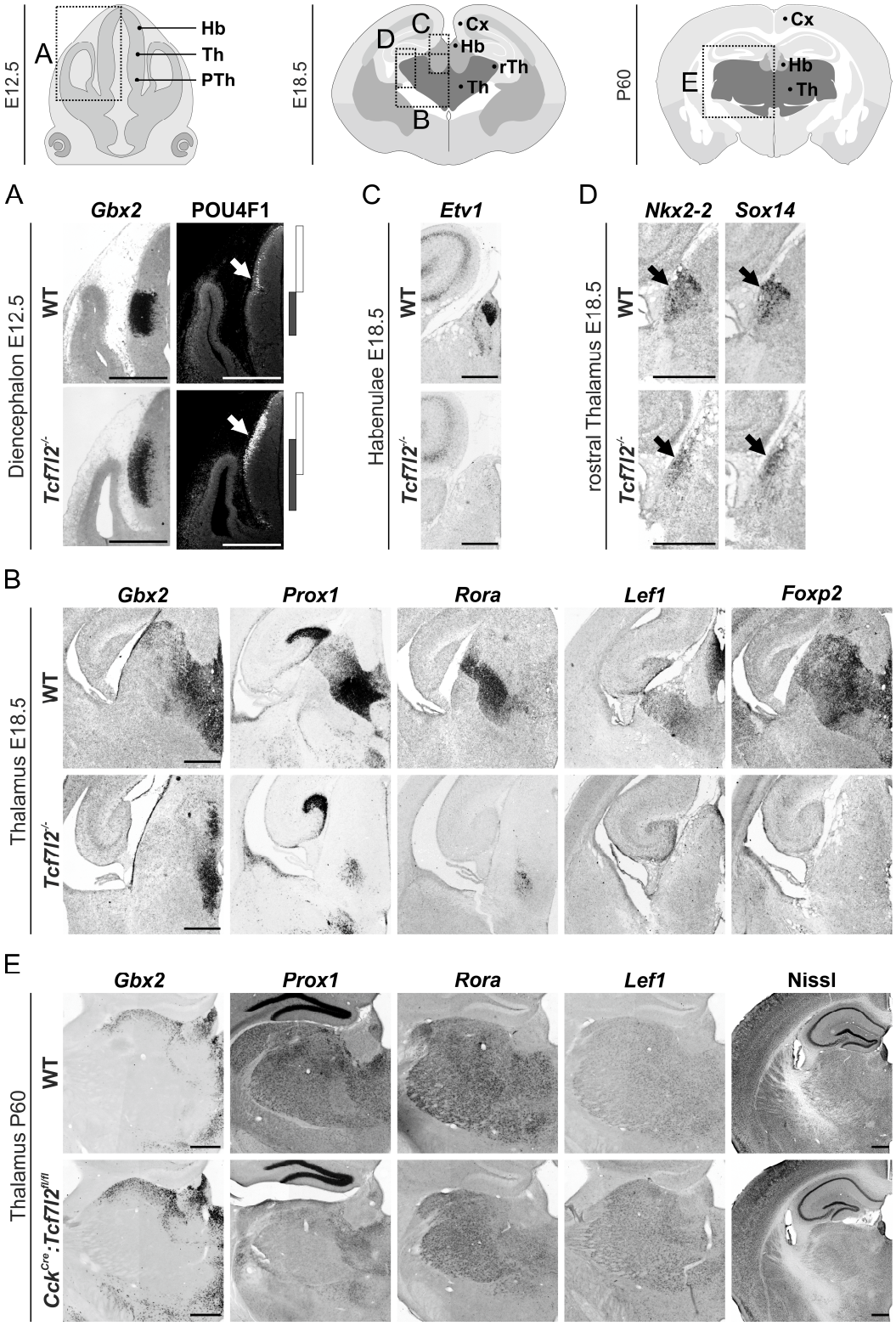


**Figure 2. TCF7L2 is indispensable for maintaining thalamic and habenular molecular identities throughout development. (A)** *In situ* hybridisation staining with a *Gbx2* probe (early marker of the thalamus) and immunofluorescent staining of POU4F1 (early marker of the habenula) in E12.5 coronal brain sections. Both markers are expressed in *Tcf7l2*$^{-/-}$ embryos at

this age, but the *Gbx2*-positive region and POU4F1-positive region spread into each other's territory (emphasised by bars). **(B)** *In situ* hybridisation staining with *Gbx2, Prox1, Rora, Lef1* and *Foxp2* probes (markers of caudal thalamus regions) in E18.5 coronal brain sections. The expression of these markers is either abolished, or drastically reduced in *Tcf7l2*$^{-/-}$ embryos at this age. **(C)** *In situ* hybridisation staining with *Etv1* probe (marker of the habenula) on E18.5. The expression of this marker is abolished in *Tcf7l2*$^{-/-}$ embryos at this age. **(D)** *In situ* hybridisation staining with *Nkx2-2* and *Sox14* probes (rTh markers) on E18.5. The expression of these markers is retained in *Tcf7l2*$^{-/-}$ embryos, although *Nkx2-2*- and *Sox14*-positive areas spread along the lateral wall of the thalamic region. **(E)** *In situ* hybridisation staining with *Gbx2*, *Prox1*, *Rora* and *Lef1* probes (markers of thalamic subregions) and Nissl staining in P60 coronal brain sections of *Cck*$^{Cre}$*:Tcf7l2*$^{fl/fl}$. The expression of *Gbx2* and *Lef1* shows little change, the expression of *Rora* is significantly lower in the medial part of the thalamus. The level of *Prox1* mRNA is reduced throughout most of the thalamus. Approximate fields of observation in the coronal planes are marked by boxes on the brain outlines above the photographs. Cx, cortex; Hb, habenula; PTh, prethalamus; rTh, rostral Thalamus; Th, thalamus. Scale bars represent 0.5 mm.

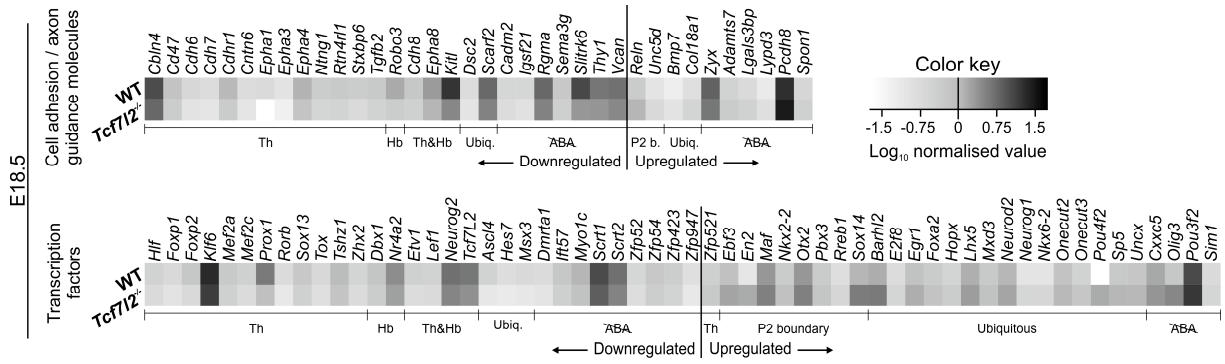


**Figure 3. TCF7L2 regulates developmental programs in the thalamo-habenular region presumably directly and *via* region-specific transcription factors.** Heatmaps of $\log_{10}$ transformed RPKM transcript levels of differentially expressed genes from overrepresented groups of cell adhesion molecules, axon guidance molecules and transcription factors, and their localisation in the brain (assessed in ABA). The knockout of *Tcf7l2* reduces the expression of thalamus and habenula-specific developmental genes. Th, thalamus-specific genes; Hb, habenula-specific genes; Th&Hb, genes expressed in thalamus and habenula; Ubiquitous, genes ubiquitously expressed throughout the brain; ~~ABA~~, genes whose spatial expression is not available at Allen Brain Atlas; P2 boundary, genes expressed at the boundary of prosomere 2.

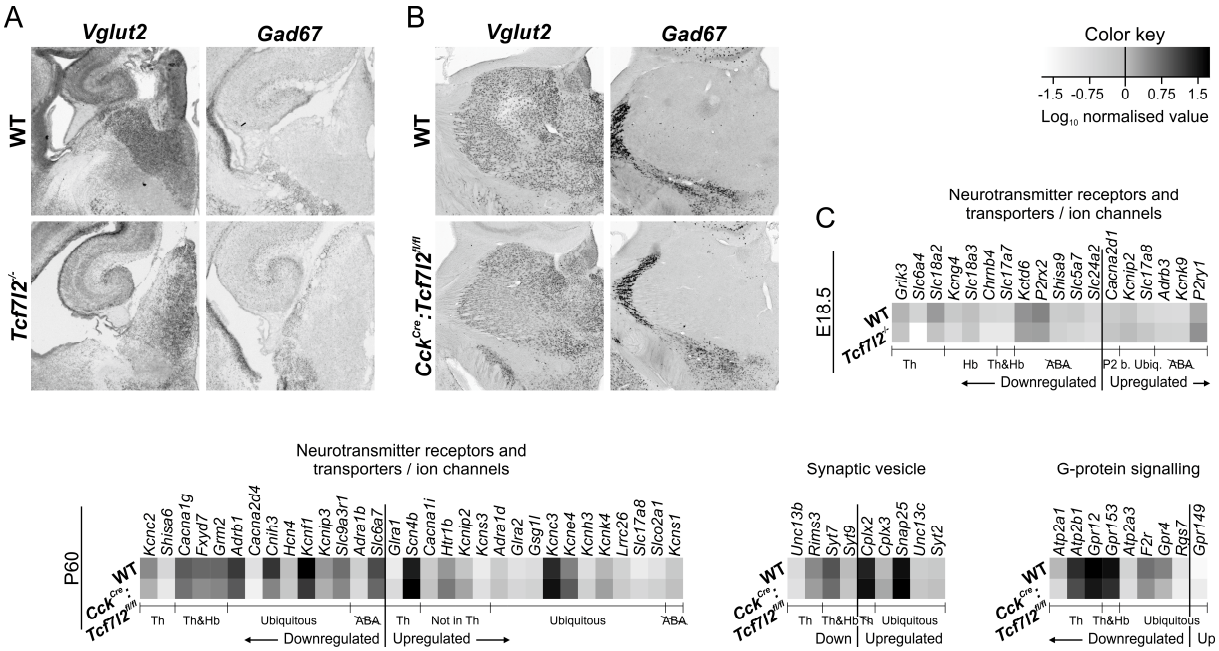


**Figure 4. TCF7L2 is required for the expression of molecular terminal markers of thalamic excitability, but not glutamatergic identity.** *In situ* hybridisation staining with *Vglut2* (marker of glutamatergic neurons) and *Gad67* (marker of GABAergic neurons) in E18.5 **(A)** and P60 coronal brain section **(B)**. E18.5 *Tcf7l2*$^{-/-}$ embryos and P60 *Cck*$^{Cre}$*:Tcf7l2*$^{fl/fl}$ mice retain predominant glutamatergic identity in the thalamic area. **(C)** Heatmaps of $\log_{10}$ transformed RPKM transcript levels of differentially expressed genes from overrepresented groups of ion-channels, neurotransmitter receptors and transmitters, G-proteins and synaptic vesicle proteins, and their localisation in the brain (assessed in ABA). Postnatal loss of TCF7L2 reduces the expression of thalamus-specific excitability genes. Th, thalamus-specific genes; Th&Hb, genes expressed in thalamus and habenula; Ubiquitous, genes ubiquitously expressed throughout the brain; ~~ABA~~, genes whose spatial expression is not available at Allen Brain Atlas; P2 boundary, genes expressed at the boundary of prosomere 2; ~~Th~~, genes specifically not expressed in thalamus.

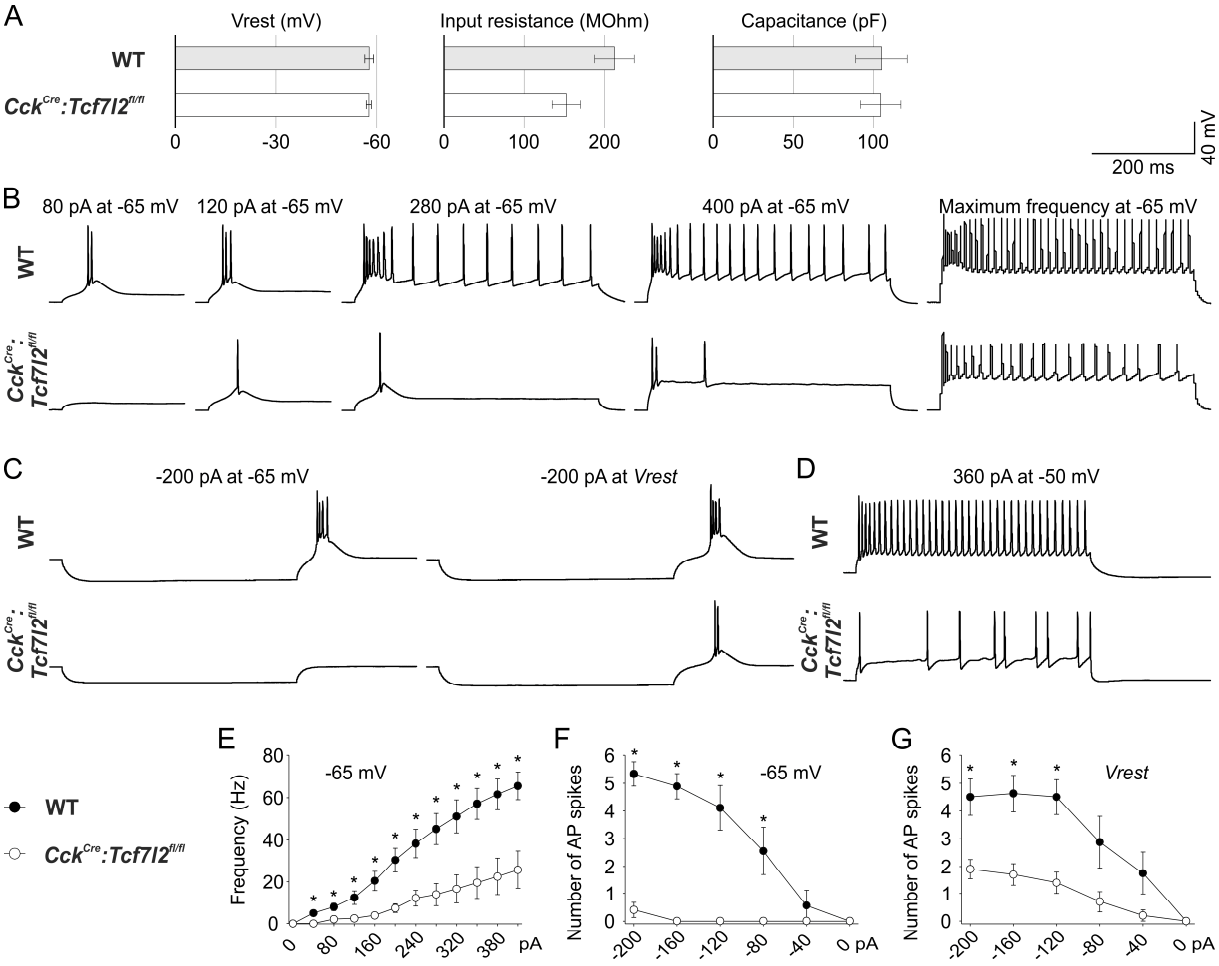


**Figure 5. TCF7L2 is necessary postnatally for the development of thalamocortical burst and tonic firing patterns. (A)** Basic electrical properties of cell membrane measured in VB neurons in brain slices. Resting potential, input resistance and membrane capacitance are not significantly changed in *Cck$^{Cre}$:Tcf7l2$^{fl/fl}$* mice. Representative traces from whole-cell patch-clamp recordings from VB neurons in brain slices at -65 mV membrane potential and increasing depolarizing current inputs (burst and tonic spikes) **(B)**, at -65 mV or the resting membrane potential (V*rest*, ~ -57 mV) and hyperpolarizing current inputs (rebound bursts of spikes) **(C)**, and at -50 mV membrane potential and depolarizing current inputs (tonic spikes) **(D)**. **(E)** Frequency of spikes evoked by increasing depolarizing currents at -65 mV, as in (B). Number of spikes per a rebound burst at -65mV **(F)** or at the resting membrane potential (*Vrest*) **(G)**, as in (C). In *Tcf7l2* mutant neurons, the frequency of spikes evoked at -65 mV membrane potential is much lower, and rebound bursts of spikes are virtually absent at this condition or are lower

in number at the resting membrane potential. Tonic spikes are evoked at -50 mV membrane potential, but their frequency is significantly lower in *Tcf7l2* mutant neurons.